

Supplementary Information for

Structure-Guided Engineering of the Affinity and Specificity of CARs Against Tn-Glycopeptides

Preeti Sharma^{a,1}, Venkata V.V.R. Marada^a, Qi Cai^a, Monika Kizerwetter^a, Yanran He^b,
Steven P. Wolf^b, Karin Schreiber^b, Henrik Clausen^c, Hans Schreiber^b, David M. Kranz^{a,1}

Corresponding authors: Preeti Sharma, David M. Kranz
Email: sharma39@illinois.edu , d-kranz@illinois.edu)

^aDepartment of Biochemistry and Cancer Center at Illinois, University of Illinois, Urbana, IL 61801, USA

^bDepartment of Pathology and Committee on Immunology, The University of Chicago, Chicago, IL 60637, USA

^cCopenhagen Center for Glycomics, University of Copenhagen, Copenhagen, Denmark

This PDF file includes:

Figures S1 to S8
Table S1
SI References

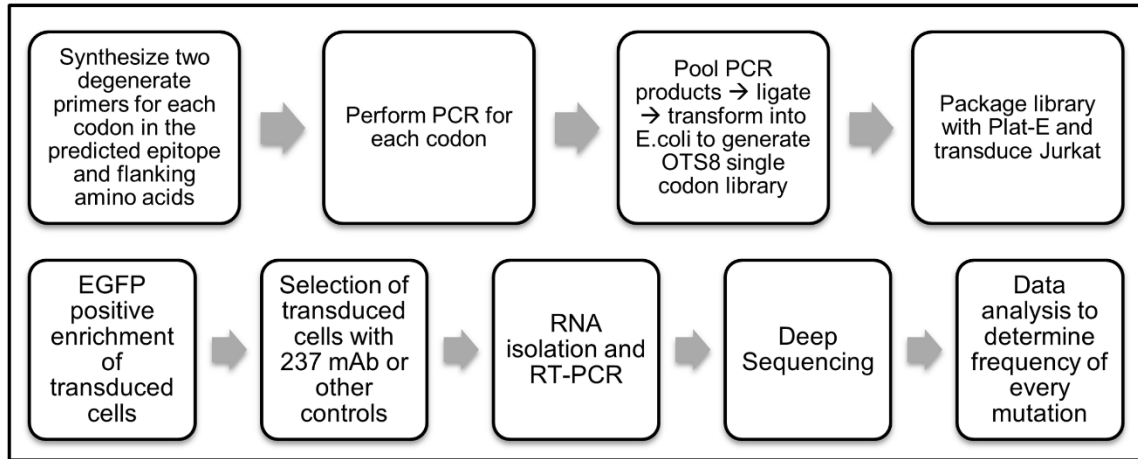


Fig. S1. Flow chart of deep mutational scan of the 237 epitope

Various steps required to conduct deep mutational scan of 237 epitope on OTS8 protein are listed.

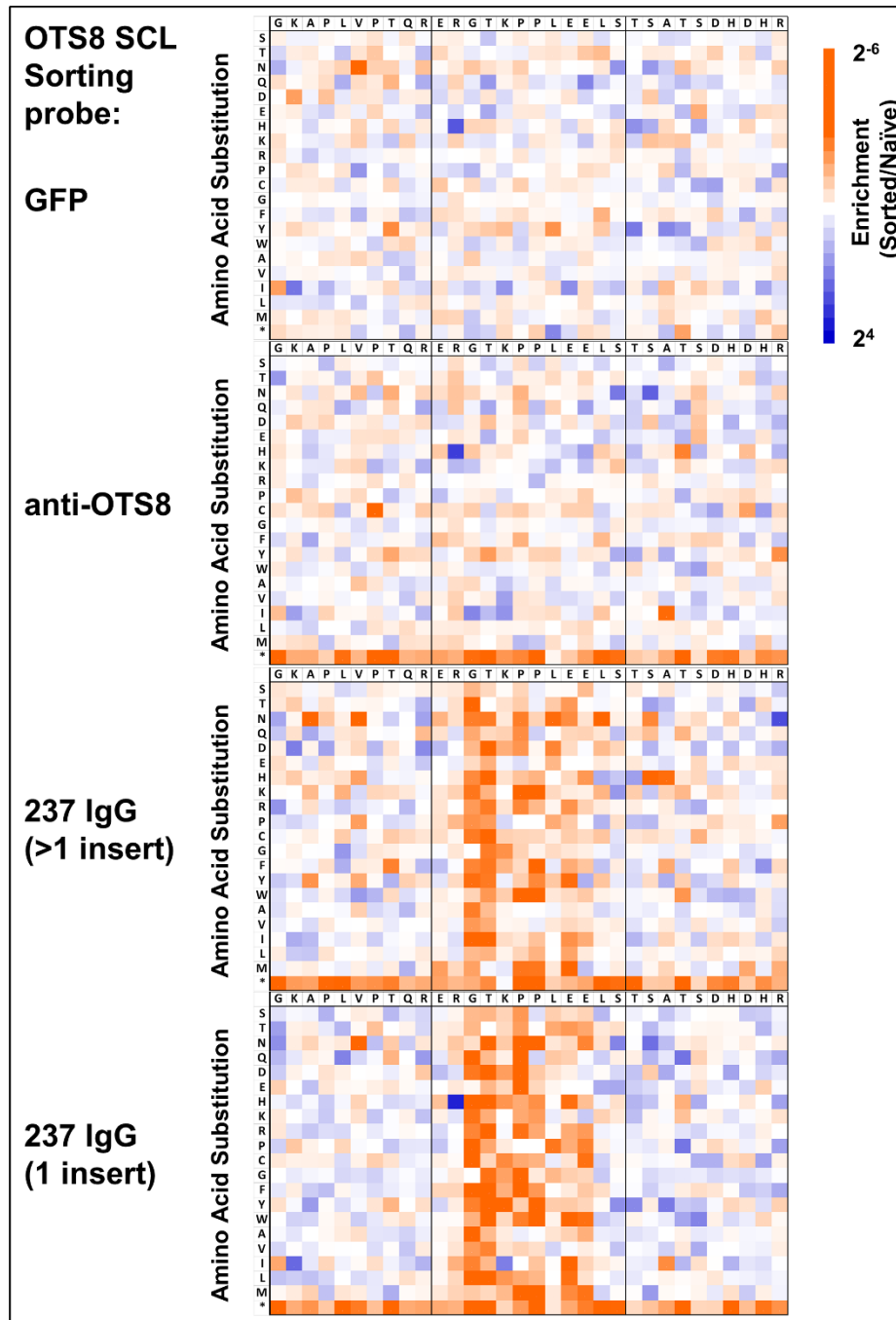


Fig. S2. Sequence fitness landscape of 237 epitope under different sorting conditions

Heat maps representing deep mutational scan of OTS8 peptide based on selection of single codon libraries (SCL) with GFP, anti-OTS8 and 237 IgG are shown. While collecting populations bound to 237 IgG, populations exhibiting low and high fluorescence (above background) were collected, corresponding to 1 or >1 gene insertion in Jurkat. Enrichment or depletion of substitutions was calculated relative to naïve (unselected) libraries as a \log_2 ratio. Resultant enrichment scores were plotted on a color-coded scale ranging from $\leq 2^{-6}$ (orange) to $\geq 2^4$ (blue). Stop codon is indicated by *.

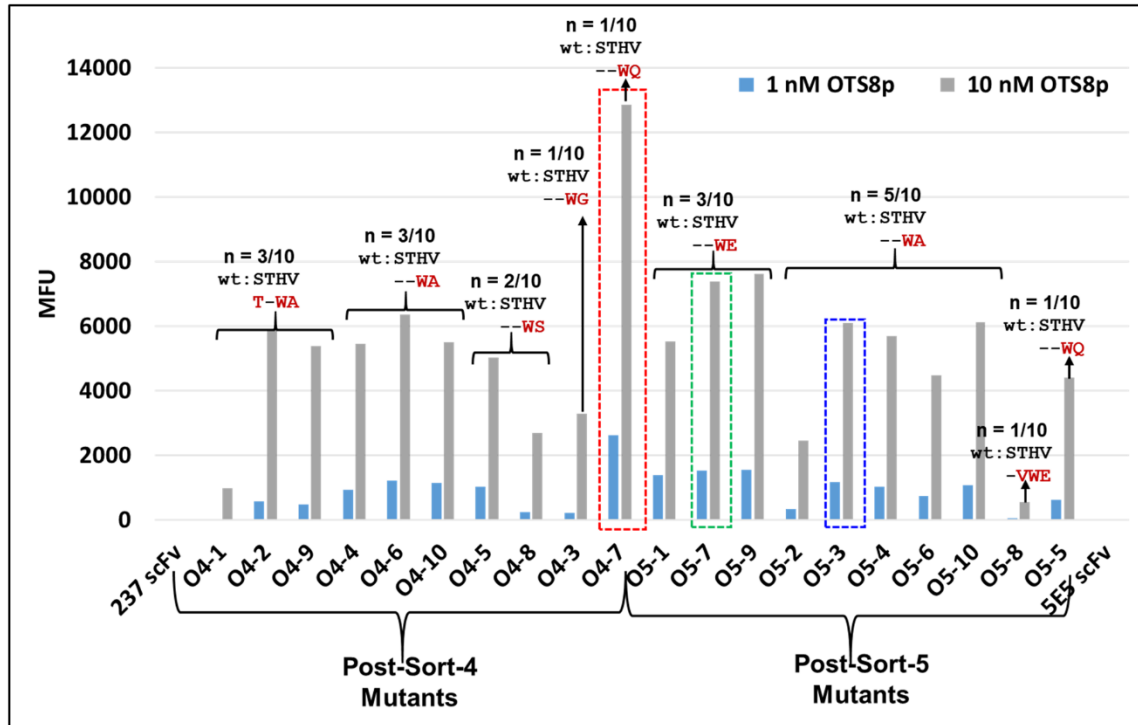


Fig. S3. Binding analysis of mutants isolated after 4 or 5 flow cytometry sorts with Tn-OTS8 peptide from the pooled CDR libraries of the yeast displayed 237 scFv

Yeast displayed 237 scFv, 5E5 scFv and twenty 237 scFv mutants isolated after sort-4 and 5 of Tn-OTS8 peptide selected libraries were stained with 1 or 10 nM Tn-OTS8 peptide and analyzed by flow cytometry. Respective mean fluorescence units (MFUs) for each mutant, and 5E5 scFv were plotted on Y-axis, for comparison with wild-type 237 scFv. In addition, plasmid DNA was isolated from each clone to determine the kind of mutation(s), and frequency of mutation(s) (n). The sequence of wild-type (wt) and mutated residues is shown in black and maroon, respectively. Mutants selected for further analysis are shown in dotted boxes.

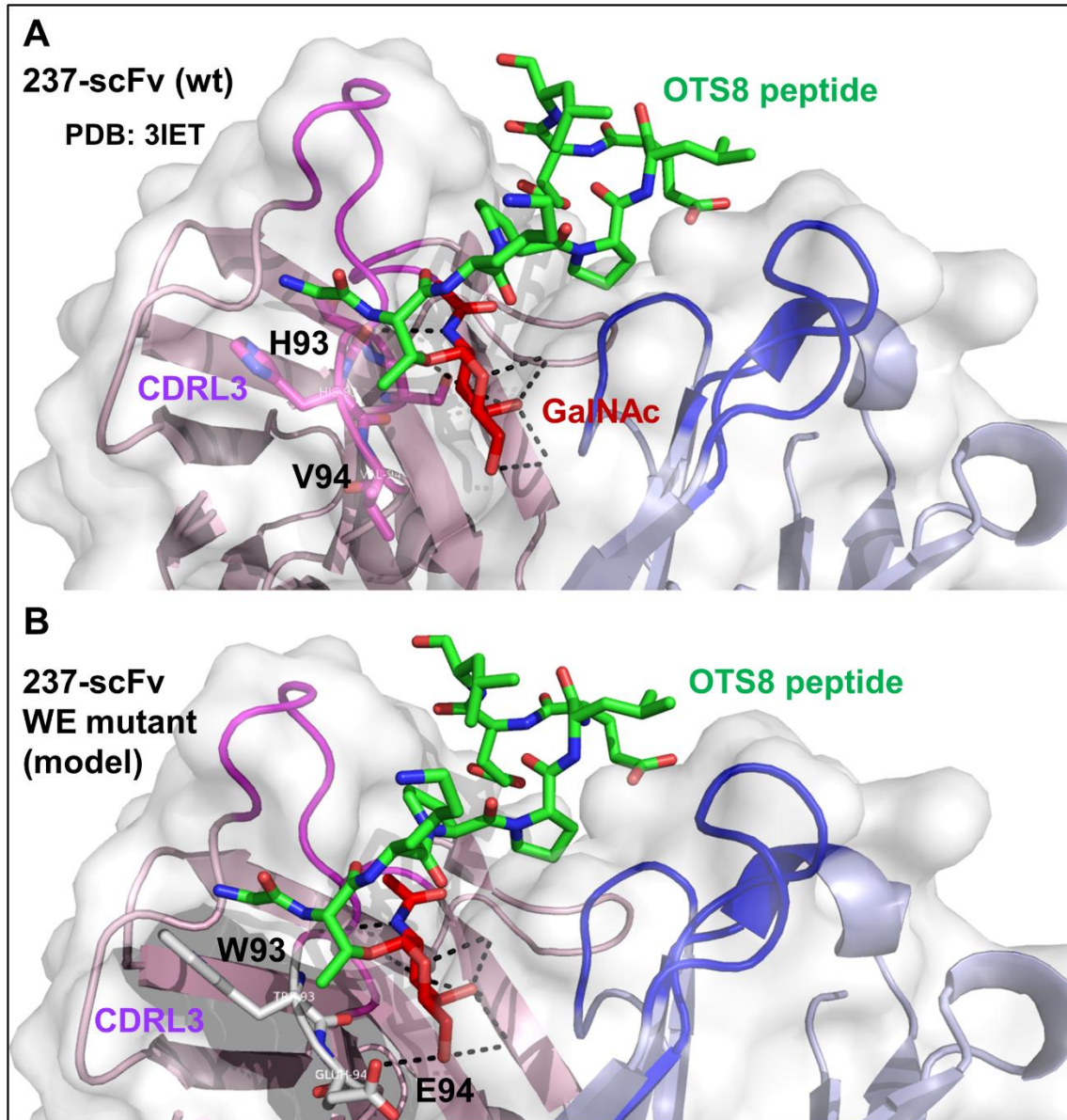


Fig. S4. Modeling WE mutation in the co-crystal structure of 237 IgG with Tn-OTS8 peptide

In order to gain insight into the possible mechanism because of which WE mutation imparted a 30-fold increase in affinity compared to the parent 237 scFv, the WE mutations were substituted in the crystal structure of 237 IgG with OTS-8 glycopeptide (PDB: 3IET) using Pymol. Pymol software was used to predict an additional polar contact between 237 and GalNAc due to the WE mutations (**B**), compared to wild-type residues (**A**).

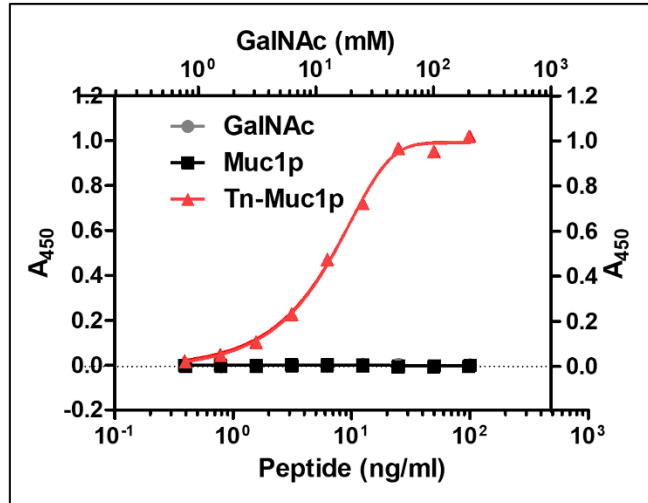


Fig. S5. Binding of enzymatically glycosylated MUC1 peptide to 5E5 antibody

To assess glycosylation of MUC1 peptide, various concentrations of the sugar (GalNAc), or unglycosylated or glycosylated MUC1 peptide (MUC1p or Tn-MUC1p) were coated on wells of an ELISA plate. After blocking with PBS+10% BSA, glycosylation of MUC1 peptide was confirmed by binding to 5E5 antibody (1 $\mu\text{g/ml}$) (mouse), detected by goat anti-mouse HRP. Absorbance at 450 nm (A_{450}) was recorded after formation of a colorimetric product by the reaction catalyzed by HRP in the presence of TMB substrate.

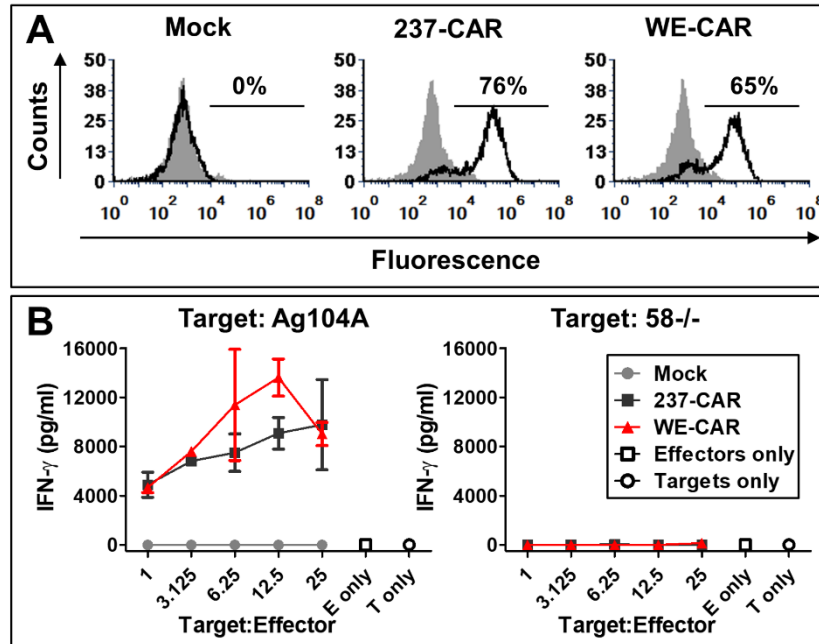


Fig. S6. Activity of T Cells Expressing 237 CAR and 237 high affinity CAR

(A) Total T cells from C57/BL6 mice were mock-transduced or transduced with 237-CAR or high affinity variant, WE-CAR. To assess transduction efficiency, cells were stained with streptavidin-PE only (gray) or, 50 nM Tn-OTS8 peptide tetramer made with streptavidin-PE (black). Transduction efficiencies are indicated as %. **(B)** To assess activation, mock, 237-CAR or WE-CAR transduced T cells were co-cultured with Ag104A, or 58^{-/-} (negative control) cell lines at various target-to-effector ratios for 24 hours at 37°C, 5% CO₂. After 24 hours, the amount of IFN- γ released in the supernatants under each co-culture condition was measured by ELISA.

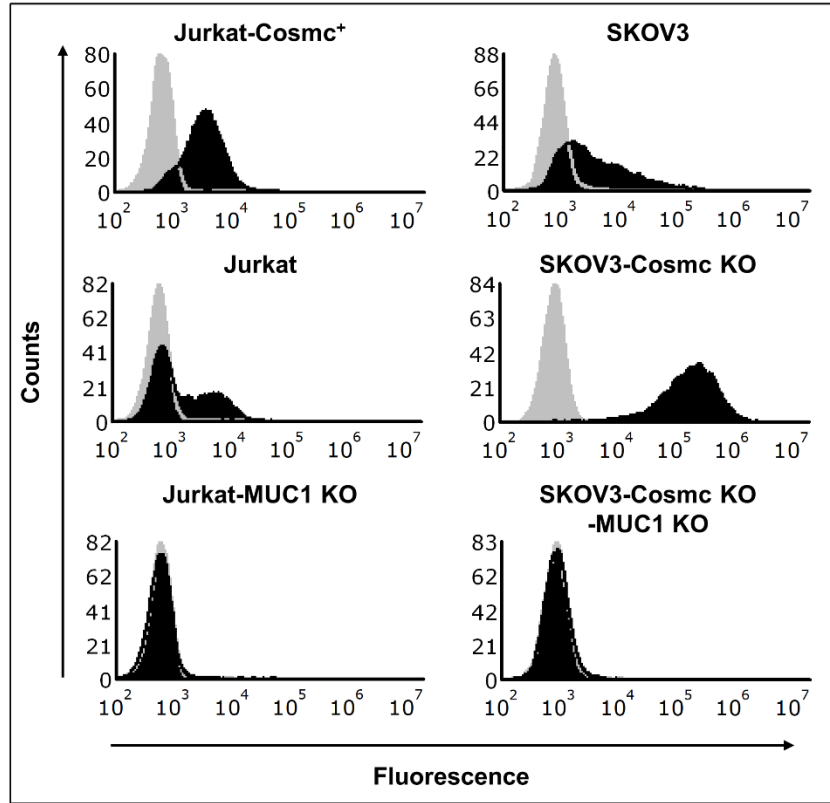


Fig. S7. Confirmation of MUC1-knock out cell lines by flow cytometry

Cell lines were stained with anti-MUC1 antibody (rabbit) (Clone HMFG2, Abcam), followed by fluorophore-linked goat anti-rabbit IgG to measure total MUC1 levels on various cell lines.

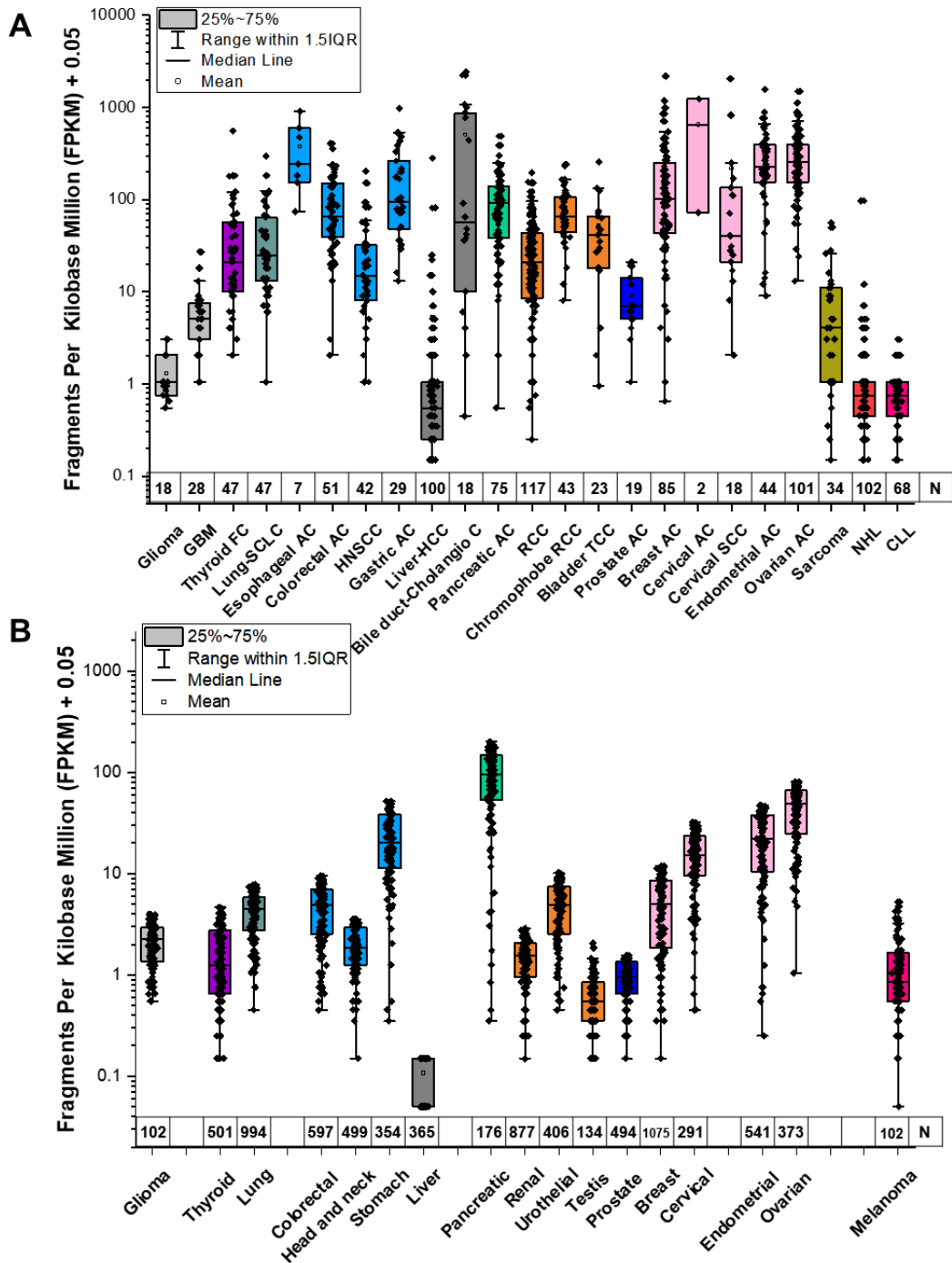


Fig. S8. MUC1 RNA expression across cancers

Expression of MUC1 across various human cancers was assessed by analyzing RNAseq data deposited in EMBL-EBI (A) (1) and TCGA (B) databases. TCGA dataset for MUC1 expression was extracted from Human Protein Atlas (2). GBM, glioblastoma multiforme; FC, follicular carcinoma; SCLC, squamous cell lung carcinoma; AC, adenocarcinoma; HNSCC, head and neck squamous cell carcinoma; HCC, hepatocellular carcinoma; RCC, renal cell carcinoma; TCC, transitional cell carcinoma; SCC, squamous cell carcinoma; NHL, non-Hodgkin lymphoma; CLL, chronic lymphocytic leukemia.

Table S1. Theoretical and expected sizes of various 3- and 4-codon CDR libraries in 237 scFv

Nine CDR libraries were constructed in the CDRs of 237 scFv, with either 3 or 4 residues mutated at a time. Each library was transformed into electrocompetent yeast, and approximate library size was calculated based on observed transformation efficiency. Observed and theoretical library sizes have been tabulated.

| Library (Loop - Targeted residues) | Library size obtained (Based on colony count) | Theoretical size |
|------------------------------------|---|-----------------------------|
| CDRL1 - HSNG | 4.2×10^7 | $(32)^4 = 1.05 \times 10^6$ |
| CDRL1 - GNTY | 1.7×10^8 | $(32)^4 = 1.05 \times 10^6$ |
| CDRL2 - KVS | 7.1×10^7 | $(32)^3 = 3.3 \times 10^4$ |
| CDRL3 - STHV | 2.6×10^7 | $(32)^4 = 1.05 \times 10^6$ |
| CDRH1 - DAW | 1×10^8 | $(32)^3 = 3.3 \times 10^4$ |
| CDRH2 - EIRN | 2×10^7 | $(32)^4 = 1.05 \times 10^6$ |
| CDRH2 - NKAN | 1.3×10^7 | $(32)^4 = 1.05 \times 10^6$ |
| CDRH2 - NNHE | 1×10^8 | $(32)^4 = 1.05 \times 10^6$ |
| CDRH3 - KVR | 7.1×10^7 | $(32)^3 = 3.3 \times 10^4$ |

SI References

- Petryszak R, Keays M, Tang YA, Fonseca NA, Barrera E, Burdett T, Fullgrabe A, Fuentes AM, Jupp S, Koskinen S, Mannion O, Huerta L, Megy K, Snow C, Williams E, Barzine M, Hastings E, Weisser H, Wright J, Jaiswal P, Huber W, Choudhary J, Parkinson HE, & Brazma A (2016) Expression Atlas update--an integrated database of gene and protein expression in humans, animals and plants. *Nucleic acids research* 44(D1):D746-752.
- Uhlen M, Zhang C, Lee S, Sjostedt E, Fagerberg L, Bidkhori G, Benfeitas R, Arif M, Liu Z, Edfors F, Sanli K, von Feilitzen K, Oksvold P, Lundberg E, Hober S, Nilsson P, Mattsson J, Schwenk JM, Brunnstrom H, Glimelius B, Sjoblom T, Edqvist PH, Djureinovic D, Micke P, Lindskog C, Mardinoglu A, & Ponten F (2017) A pathology atlas of the human cancer transcriptome. *Science* 357(6352).